Modelling of magnetisation processes in transformer steel sheets

MICHAŁ SIERŻĘGA ^{ID} [✉], WITOLD MAZGAJ ^{ID}

Department of Electrical Engineering, Cracow University of Technology
24 Warszawska str., 31-155 Kraków, Poland
e-mail: ✉*michal.sierzega@pk.edu.pl, pemazgaj@cyfronet.pl*

Abstract: This study describes a method that allows the modelling of magnetisation processes in transformer steel sheets for any direction of the magnetic field strength. In the proposed approach, limiting hysteresis loops for the rolling and transverse directions were used. These loops are modified depending on the magnetisation angle between the direction of the field strength vector and rolling direction. For this purpose, unique correction coefficients, which are functions of the magnetisation angle, were applied for both hysteresis loops. An algorithm for determining the limiting hysteresis loops for any magnetisation angle is presented herein. The calculation results for several cases of magnetisation were compared with the measured hysteresis loops.

Key words: Goss texture, hysteresis loop, magnetisation process, modelling, transformer core, transformer steel sheet

1. Introduction

Calculations of losses in transformer cores, especially of medium- and high-power, is still an important issue; in recent years, this problem has been discussed in [1–3]. The highest magnetic flux density occurs in the inner parts of corners and T-joint points of the transformer cores. It should be noted that the magnetic field lines in these areas are parallel neither to the rolling direction nor to the transverse direction. A significant difficulty in numerical calculations of losses is the consideration of the non-linearity of the transformer core and, above all, the magnetic hysteresis. Professional software allows one to take into account the non-linear but unambiguous magnetisation characteristics, which is discussed e.g. in [4, 5]. However, direct consideration of the magnetic hysteresis by introducing a certain model of this phenomenon into

the field distribution equations is not possible in methods such as the finite difference method, and the finite element method, because these methods are based on the differential form of the Maxwell's equations. The introduction of the hysteresis model into the equations of the magnetic field distribution is possible in the equivalent reluctance network method, which is based on Maxwell's equations in the integral form or using a significant modification of this method described in [6, 7].

The lines of the magnetic field in the transformer cores are mostly parallel to the rolling direction (RD). It refers to the columns and yokes of these cores; therefore, the magnetic field can be treated as a one-dimensional field. However, the lines of the magnetic field in the corners and T-joint points of three-phase transformers are not parallel to the RD, similar to the overcurrent states of the transformers, because a significant leakage flux can close through the air. Consequently, the magnetic field in these regions should be considered a two-dimensional field (Fig. 1). Calculations of the field distribution in corners and in T-joint points are still an important issue because in these areas, the heating of the core is more intense compared to the part of the core where the magnetic field can be treated as a one-dimensional field. It is important in medium- and high-power transformers. Changes in the flux density and field strength differ from each other because of the hysteresis phenomenon and anisotropy of the transformer sheets, and the vectors of these magnetic quantities are usually not co-linear.
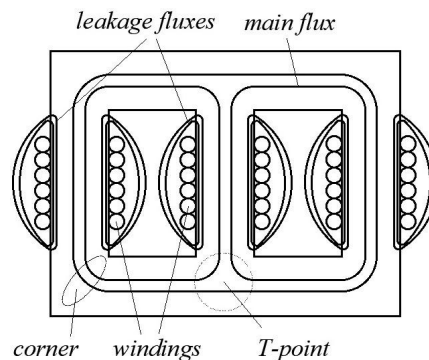

Fig. 1. Part of a transformer core with examples of field strength directions

Note that the magnetisation characteristics for directions other than RD have a shape that is significantly different relative to the shape of a "classic" hysteresis loop (Fig. 2) [8–10]. This causes significant difficulties in the calculation of the magnetic field distribution in the aforementioned regions of the transformer cores because the hysteresis loops for particular directions of the possible magnetisation processes differ from each other.

The measurements of hysteresis loops along different magnetisation directions were made using the Epstein frame at a frequency of 3 Hz, which allows the effect of eddy currents to be neglected. Strips for the Epstein frame were cut from the tested transformer sheet at assumed angles with respect to the rolling direction.

The scientific literature contains papers that present hysteresis loops of the transformer sheets for directions other than the RD; however, most often, these loops are a result of measurements, not calculations using some model of magnetisation processes occurring in these sheets.
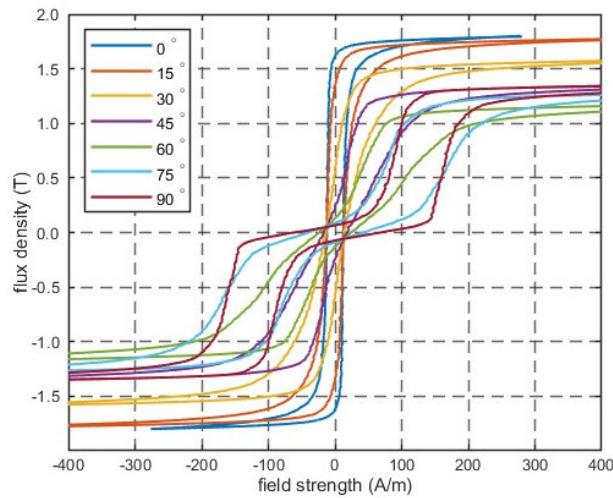
Fig. 2. Hysteresis loops of the transformer sheet type M120-27S measured for seven
magnetisation directions every 15 degrees

2. Magnetisation processes in transformer steel sheets

Transformer steel sheets are produced as grain-oriented sheets, and the Goss texture is a characteristic feature. Each iron crystal of the transformer sheet is cubic in shape and has three easy magnetisation axes (Fig. 3) [11–14]. One is parallel to the rolling direction, and the two axes are inclined at an angle of 45° with respect to the transformer sheet plane. This causes these sheets to be most easily magnetised along the rolling direction. In other directions, the magnetisation properties are significantly worse. When the direction of the field strength is not parallel to the RD,
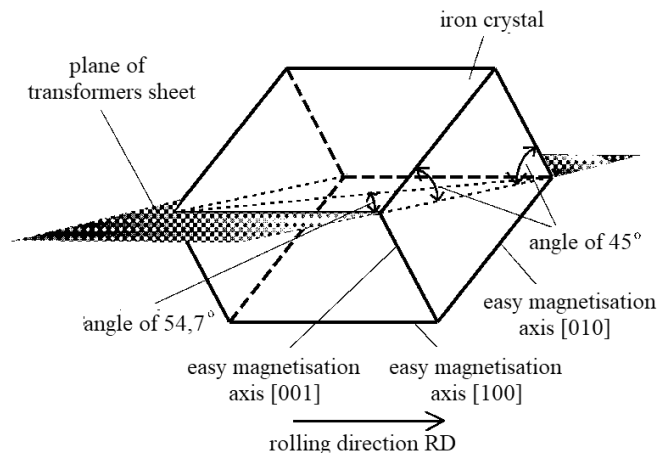

Fig. 3. Iron crystal in a transformer sheet with the Goss texture

magnetisation processes occur in varying degrees along each easy magnetisation axis. It should be noted that the magnetisation process in iron crystals first occurs along the easy magnetisation axes [100], [010], [001]. Note that the [010] and [001] axes are magnetically equivalent.

In typical transformer sheets, the process of rotation of the resultant flux density vectors of individual magnetic domains towards the direction of the magnetic field strength begins when the field strength is several hundred A/m. Therefore, for lower values of field strength, the resultant flux density vector at any point on the given transformer sheet can be treated as the sum of the flux densities along the RD ([100]) and along the transverse direction (TD), where the value of this flux density is the sum of the flux densities along the axes [010] and [001] multiplied by $\cos 45°$. The measured flux density value for a certain magnetisation direction is the projection of the resultant flux density vector in the magnetisation direction. For both the RD and TD, the flux density and field strength vectors are co-linear. The value and direction of the resultant flux density vector cannot be determined directly. Changes in its value and direction depend on the direction of magnetisation [8]. If any magnetisation process occurs at an angle less than 54.7 with respect to the RD, the flux density along the TD initially increases as well. Because the algebraic sum of the flux densities along the RD and TD cannot be higher than the saturation flux density of the given transformer sheet, the flux density along the TD decreases and tends to zero when the field strength increases. When the magnetisation angle is greater than 54.7 with respect to the RD, the flux density value along the RD also increases initially. At high field strength values, the direction of the resultant flux density vector is closer to the TD.

It should be emphasised that domains which create 180-degree walls are rebuilt into domains which form the 90-degree walls [10]. The flux density vectors (or magnetisation vectors) of 'new' domains are parallel to one of the axes [010], [001]. During this domain rebuilding the resultant flux density of the whole sheet sample increases relatively slowly, and the flux density begins to increase faster after the end of this process.

3. Modelling of the magnetisation process in transformer sheets

The domain structure and its changes in the transformer steel sheets are frequently used to model the magnetisation process in these sheets. In previous studies [15, 16], the dependence between the magnetic properties of the transformer sheets and their domain structure was discussed; however, the authors of these papers did not propose how to determine the hysteresis curves for any direction of the magnetisation process. Similar comments apply to the works [17, 18], which proposed modelling the magnetisation process for two specific directions, that is, for the rolling and transverse directions. However, the most useful of the proposals so far is the modelling method of the magnetisation processes presented in [10], in which the hysteresis loops measured and calculated for several magnetisation directions on the sheet plane are compared. However, this study does not present a method for determining partial hysteresis loops for any direction of the magnetisation process. Proposals on modelling magnetisation processes using tensor relationships were presented in [19, 20]; however, such an approach does not allow the correction of model magnetisation processes for any direction of the field strength. In [21], a hysteresis operator for the simulation of Goss-textured ferromagnetic materials was proposed, which is based on the classic Stoner–Wohlfarth model.

In the proposed approach of modelling the magnetisation process in the transformer sheets, rotations of the flux density vectors towards the field strength direction are neglected because such cases occur for relatively high field strength values. This implies that the changes in the flux density only occur along three easy magnetisation axes of the iron crystals. The proposed method refers to a static hysteresis loop. The impact of eddy currents is often included in calculations by introducing an additional eddy current resistive network related to the magnetic field network [22–24].

The proposed model enables calculation of the magnetisation process in transformer steel sheets for any direction on the sheet plane. In further consideration, the easy magnetisation axes are denoted as axes 1, 2 and 3, respectively, and the field strength and flux density along these axes have appropriate indices. Let the direction of the magnetic field strength H_α form an angle α_H with respect to axis 1 (Fig. 4). The values of the field strength along axis 1 are equal to:

$$H_1 = \cos \alpha_H H_\alpha. \tag{1}$$

The easy magnetisation axes, 2 and 3, are magnetically equivalent; therefore, the field strength values of these axes can be written as follows:

$$H_2 = H_3 = \cos 45° \sin \alpha_H H_\alpha. \tag{2}$$

The resultant flux density occurring on the sheet plane is the vector sum of the flux densities along axes 1, 2, and 3. Because axes 2 and 3 are magnetically equivalent, it can be assumed that at an angle of $45°$ to the sheet plane, one axis of easy magnetisation exists, and the flux density along this axis, denoted as B_{23}, is the sum of flux densities along axes 2 and 3. However, it is not possible to determine the values of the resultant flux density vector on the basis of the magnetisation curves measured along the rolling and transverse direction, because changes in the flux density along the easy magnetisation axes depend on the direction of the magnetic field strength.

Depending on the direction of the field strength, a process of rebuilding the domain structure occurs in transformer sheets, which not only involves rebuilding of the 180-degree walls but also the 90-degree walls [8, 10]. The intensity of this rebuilding of the domain walls strongly depends on the angle α_H between the direction of the given field strength and the rolling direction (Fig. 4).
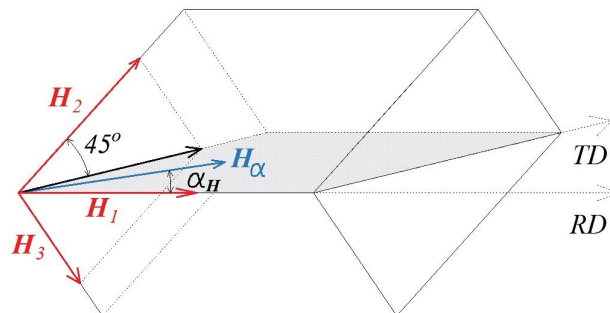

Fig. 4. Determination of the field strength value along easy magnetisation axes

The higher the angle, the greater is the intensity. However, the rebuilding process has not been sufficiently described quantitatively or qualitatively. Because of the occurrence of this process, it is not recommended to consider the magnetisation characteristics in the rolling direction, as shown in Fig. 2. When the directions of the field strength are different, some domains are under rebuilding, and they cannot be considered for the given values of the field strength. Therefore, in these cases, changes in the flux density along axis 1 should be determined separately for each direction of the magnetic field strength. These dependencies are only determined to limit the hysteresis loops for individual directions of the field strength.

The hysteresis limiting loop for each magnetisation direction should be determined because the so-called minor hysteresis loops are inside the limiting loops. The limiting hysteresis loops were determined based on the measured loop for the rolling direction (RD, axis 1) and the loop for direction 23, which was determined on the basis of measurements in the transverse direction (TD). It is assumed that when the magnetisation angle α_H increases, the flux density along axis 1 changes more slowly, that is, the same flux density value occurs for higher values of field strength H_1 with increasing magnetisation angle. For this purpose, the field strength values resulting from Formula (1) are multiplied by an appropriately selected correction coefficient w_1, which is equal to 1 for $\alpha_H = 0$ and less than 1 for magnetisation angles greater than zero:

$$H_{1\alpha} = \frac{1}{w_1} \left(\cos \alpha_H H_\alpha \pm H_{c1} \right) \mp H_{c1} , \tag{3}$$

where H_{c1} is the coercive force of the hysteresis loop along the rolling direction.

When the field strength increases, in the first component of the last formula the sign "−" occurs, and the second component has the sign "+". However, when the field strength decreases, the first component has the sign "+" and the second term has the sign "−". This note applies to all subsequent dependencies where the character "±" occurs.

A similar procedure was applied for direction 23; the correction coefficient w_{23} for this direction was equal to 1 for $\alpha_H = 90°$; for other angles, this coefficient was less than 1. The field strength $H_{23\alpha}$ along direction 23 is expressed as:

$$H_{2\alpha} = H_{3\alpha} = H_{23\alpha} = \frac{1}{w_{23}} \left(\cos 45° \sin \alpha_H H_\alpha \pm H_{c23} \right) \mp H_{c23} , \tag{4}$$

where H_{c23} is the coercive force of the hysteresis loop along direction 23, which was determined based on the hysteresis loop for the transverse direction.

To select the values of the correction coefficients w_1 and w_{23} for the given magnetisation angles, the hysteresis limiting loops should be calculated for different values of these coefficients, and the values for which the calculated limiting loops are closest to the measurement loops are selected. For this purpose, the least squares method is recommended. Figure 5 shows the correction coefficients for magnetisation angles from 0° to 90°. Determination of the coefficient w_{23} for magnetisation angles lower than 54.7° is not critical because the values of the flux density along the TD are relatively small in a significant range of changes in field strength.

The correction coefficients for the other angles are determined based on a linear approximation of the coefficients for the two angles closest to the given angle. Figure 6 shows hysteresis loops along axes 1 and 23 for several magnetisation angles α_H.

The magnetic properties of iron crystals show that the sum of flux density B_1 along axis 1 and B_{23} along axis 23 cannot be greater than the saturation flux density B_{sat}. Hence:

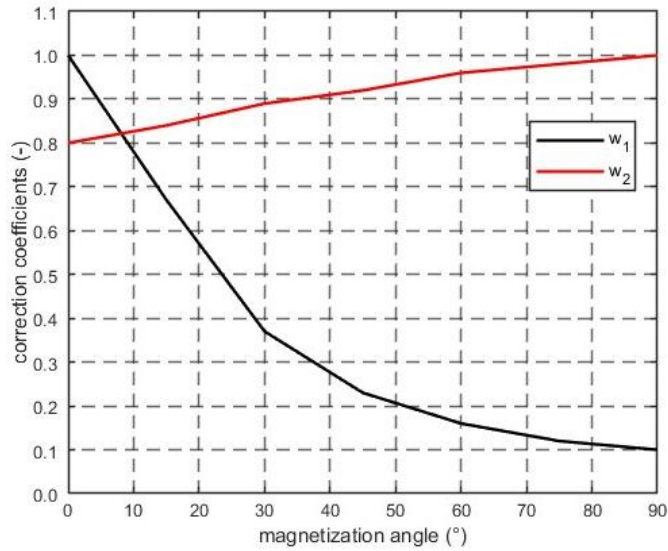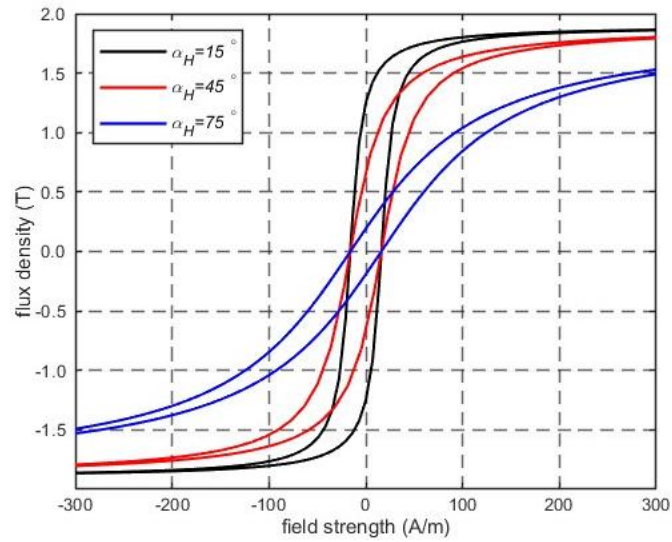$$\text{abs}(B_1) + \text{abs}(B_{23}) \leq B_{\text{sat}} \,. \tag{5}$$

Fig. 5. Values of the correction coefficients w_1 (black line) and w_{23} (red line) for several magnetisation angles
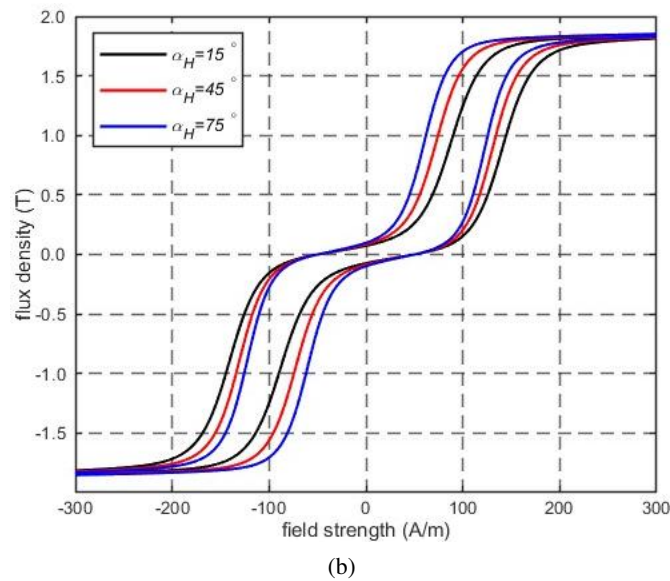

(a)

(b)

Fig. 6. Limiting hysteresis loops for several magnetisation angles α_H along: (a) axis 1; (b) axis 23

Therefore, condition (5) should be checked during the determination of the limiting loops. If the sum of the flux densities is greater than B_{sat}, then for increasing field strength values, the flux density B_{23} decreases if the magnetisation angle is less than $54.7°$; otherwise, the flux density B_1 decreases and B_{23} increases simultaneously. The algorithm used to determine the limiting hysteresis loops is illustrated in Fig. 7.

Before starting the calculations of the limiting hysteresis loop for any magnetisation angle, the following data should be entered: the measured limiting hysteresis loops $B_{RD} = f_{RD}(H_{RD})$ and $B_{TD} = f_{TD}(H_{TD})$ for both the rolling and transverse directions, the maximum value H_{max} of the field strength, an assumed field strength increase ΔH, and values of the correction coefficients w_1 and w_{23} for the given magnetisation angle. The hysteresis loop for direction 23 was determined based on the hysteresis loop measured along the transverse direction. For successive values of the field strength H_α along the given magnetisation direction, the field strengths H_1 and H_{23} were determined, and then the flux density values along these directions were determined:

$$B_1 = f_{RD}(H_{1\alpha}) = f_{RD}\left[\frac{1}{w_1}\left(\cos\alpha_H H_\alpha \pm H_{c1}\right) \mp H_{c1}\right], \tag{6}$$

$$B_{23} = \frac{1}{\cos 45°}f_{TD}(H_{23\alpha}) = \frac{1}{\cos 45°}f_{TD}\left[\frac{1}{w_{23}}\left(\cos 45° \sin\alpha_H H_\alpha \pm H_{c23}\right) \mp H_{c23}\right]. \tag{7}$$

For each value of field strength H_α, condition (5), which refers to the saturation state, should be checked. If this condition is satisfied, calculations are performed for the next value of the field strength. Otherwise:

$$B_{23} = \text{sign}(H_{23})B_{\text{sat}} - B_1 \quad \text{if} \quad \alpha_H \leq 54.7°, \tag{8a}$$

or

$$B_1 = \text{sign}(H_1)B_{\text{sat}} - B_{23} \quad \text{if} \ \alpha_H \geq 54.7°. \tag{8b}$$
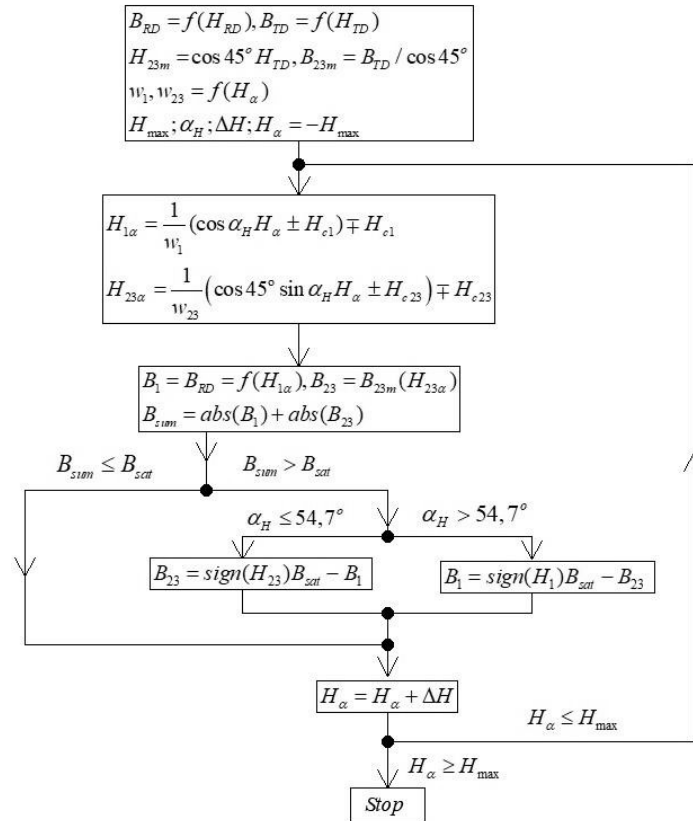

Fig. 7. Determination of the limiting hysteresis loops

4. Examples of modelling of magnetisation processes

It is necessary to determine minor hysteresis loops for any value of the magnetic field strength in the calculation of magnetisation processes in transformer steel sheets. For this purpose, the Preisach hysteresis model or the Jiles-Atherton model has been proposed for use in [25–27]. However, both models have disadvantages, as discussed in [28]. In the proposed approach to modelling the magnetisation processes, the method of approximation of hysteresis changes presented in [29] was applied. This study extensively describes how to determine minor hysteresis loops for any field strength value, and the model of the magnetisation process in transformer steel sheets can be universal when it allows the determination of changes in flux density for any value and direction of the field strength. Therefore, for magnetisation angles for which measurements have not been

performed, the correction coefficients w_1 and w_{23} should be selected such that the differences between the measured and calculated loops are as small as possible.

For the given magnetisation direction and the given value of the field strength H_α, projections of this field strength on axis 1 and direction 23 are calculated, and the flux density B_1 along axis 1 and flux density B_{23} along direction 23 are determined. Further, the value of the flux density vector B_α for a given magnetisation direction is determined as follows:

$$B_\alpha = \cos\alpha B_1 + \cos 45° \sin\alpha B_{23} . \tag{9}$$

Calculations of values B_α allow the comparison of the calculated flux densities with the measured values for the given magnetisation angle, and this is the basis for verifying the correctness of the proposed model of the magnetisation process in transformer sheets.

One of the main purposes of calculating the magnetisation processes is to determine the changes in the resultant flux density vector, particularly in the corners and T-joint points of transformer cores. This vector is the geometric sum of the flux densities along directions 1 and 23, and its length $B_{\alpha\text{res}}$ is equal to:

$$B_{\alpha\text{res}} = \frac{\cos 45° B_{23}}{\sin\alpha_{\text{res}}} , \tag{10}$$

where α_{res} denotes the angle between the direction of the resultant flux density vector and the rolling direction.

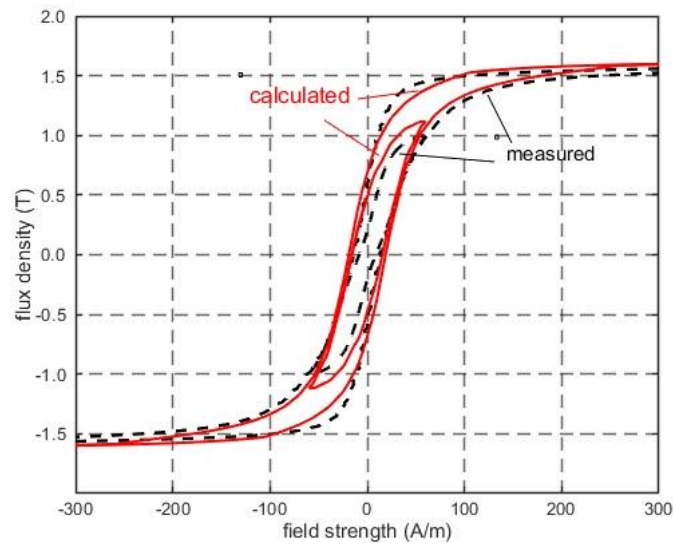The angle α_{res} on the sheet plane can be determined as follows:

$$\alpha_{\text{res}} = \arctan\left(\frac{\cos 45° B_{23}}{B_1}\right) . \tag{11}$$

Exemplary calculations were performed for the magnetisation angle of 30° and 60°. Figure 8 shows the measured and calculated limiting and minor hysteresis loops. Figure 9 shows the changes in flux density along axes 1 and 23 for the same values of magnetisation angle.
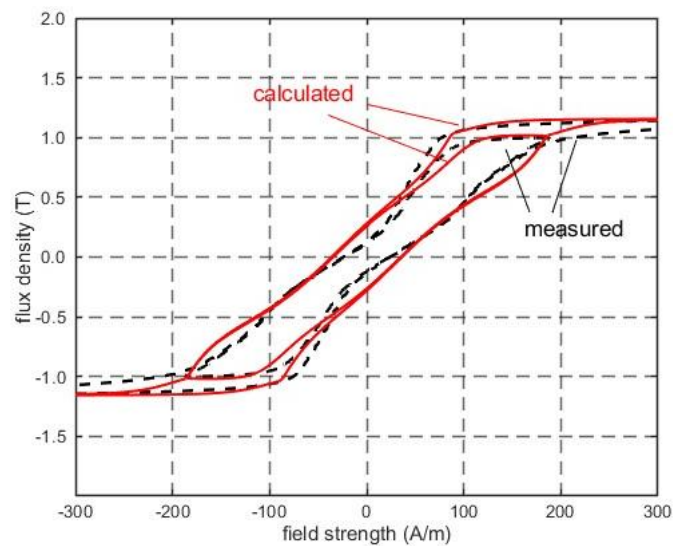
When the magnetisation angle is 30° then at the field strength of about 256 A/m ($H_1 = 221$ A/m, $H_{23} = 91$ A/m) the sum of the flux densities B_1 and B_{23} is equal to B_{sat}. The changes in the flux density B_1 along axis 1 are predominant. The flux density B_1 increases to B_{sat}, and B_{23} decreases to zero. At the magnetization angle 60°, the flux density B_1 decreases to zero, and B_{23} increases to B_{sat} when the field strength is higher than 186 A/m ($H_1 = 93$ A/m, $H_{23} = 114$ A/m). In this case, the changes in the flux density B_{23} along axis 23 have a decisive influence on this magnetization process.

Note that the flux density along the transverse direction TD on the sheet plane is equal to the flux density B_{23} multiplied by $\cos 45°$. This nature of changes in the flux densities along axis 1 (rolling direction) and axis 23, which forms an angle of 45° with the transverse direction on the sheet plane, was discussed in [8] and partially confirmed by measurements [30, 31].

When the saturation flux density B_{sat} is reached during the magnetisation process at an angle of 30° (Fig. 9(a)), the lower limiting curve B_{23r} becomes the upper curve and vice versa. After reaching the saturation state, flux density B_{23} changes according to the limiting curve B_{23r} with increasing field strength values. If the field strength starts to decrease, flux density B_{23} moves to curve B_{23d}. When the algebraic sum of flux densities B_1 and B_{23} is lower than B_{sat}, flux
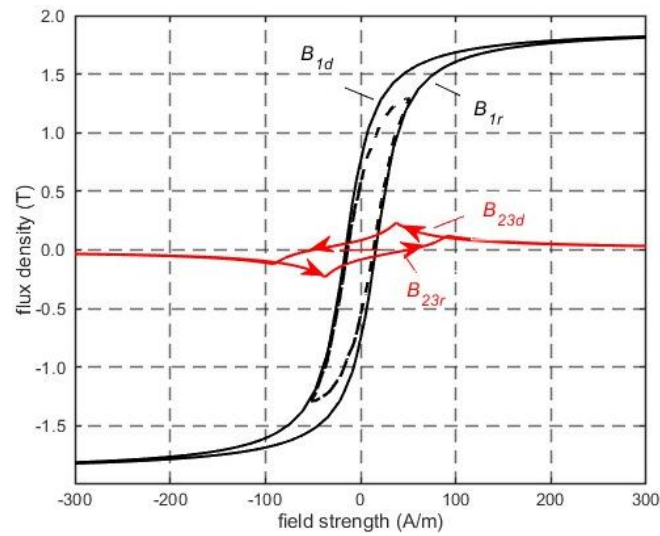
(a)

(b)

Fig. 8. Limiting and minor hysteresis loops for the magnetisation angle: (a) 30°; (b) 60°;
continuous lines – calculated loops, dashed lines – measured loops

density B_{23} changes only along the limiting curve B_{23d}. Similar changes were observed for the flux density B_1 when the magnetisation angle was 60° (Fig. 9(b)).
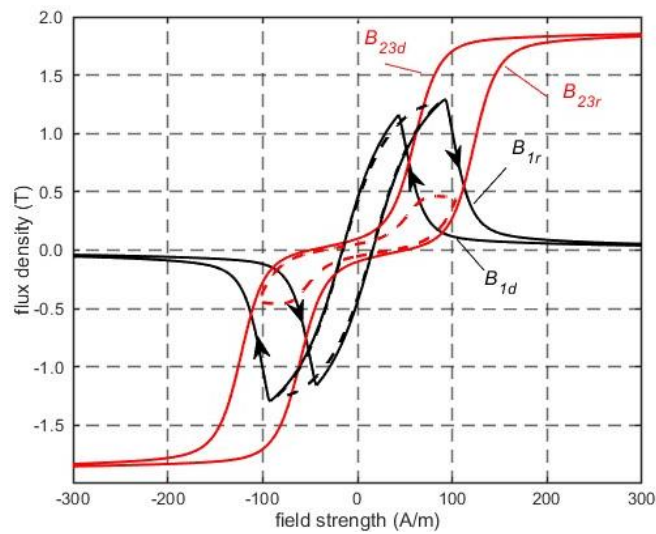
The hysteresis loops of the resultant flux densities for magnetisation angles of 30° and 60° are shown in Fig. 10. These loops differ from those calculated and measured along the

magnetisation angles, and, as mentioned earlier, the flux density along the magnetisation direction is the projection of the resultant flux density vector onto the magnetisation direction.

Certain 'teeth' that appear on the resultant hysteresis loop for the magnetisation process at an angle of 60 degrees require an explanation. These small 'teeth' appear when the sum of the flux
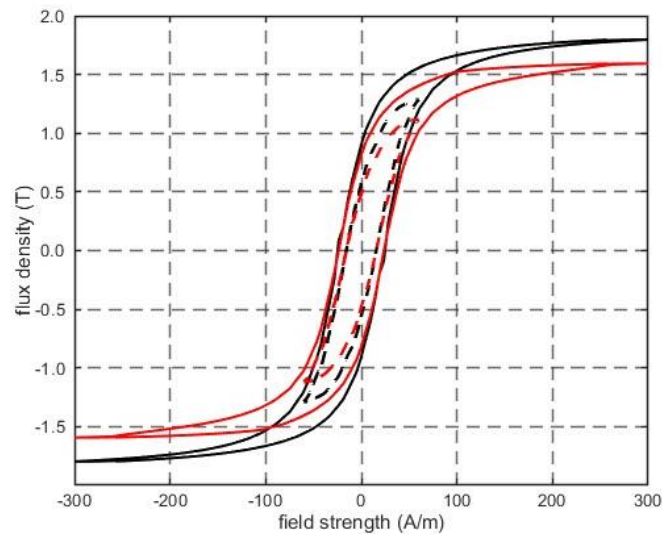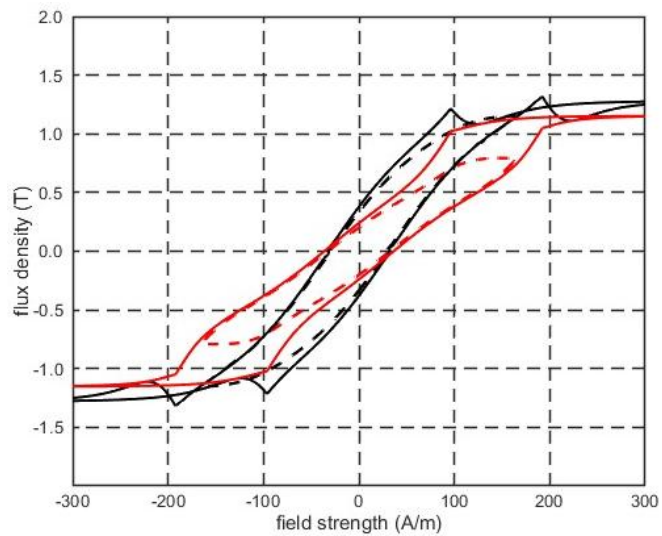

(a)

(b)

Fig. 9. Limiting and minor hysteresis loops along axes 1 and 23 for the magnetisation angle: (a) 30°; (b) 60°; B_{1r}, B_{23r} – flux densities for increasing field strength along direction 1 and 23, respectively, B_{1d}, B_{23d} – flux densities for decreasing field strength along direction 1 and 23, respectively, continuous lines – limiting hysteresis loops, dashed lines – minor loops

density in axes 1 and 23 is close to the saturation flux density. This is because B_1 decreases as soon as the sum of B_1 and B_{23} equals B_{sat}.

The direction of the resultant flux density vector is not constant and depends on the magnetic field strength. Consequently, the magnetisation process in transformer steel sheets cannot be

(a)

(b)

Fig. 10. Hysteresis loops of the resultant flux density and hysteresis loops along the magnetisation direction for the angle: (a) $30°$; (b) $60°$; black lines – calculated loops of the resultant flux density, red lines – calculated loops of the flux density along the magnetisation direction, continuous lines – limiting loops, dashed lines – minor loops

treated as the axial magnetisation when the field strength direction is different from the rolling and transverse direction. This should be taken into account during calculations of changes in flux density in the corners and T-joint points of the transformer cores, especially during estimation of losses in these areas.

5. Conclusions

The proposed modelling of the magnetisation process for any direction in the transformer sheets requires only measurements of the limiting hysteresis loops in both the rolling and transverse directions. In addition, hysteresis loops should be determined for several selected angles in order to properly determine the correction coefficients which allows the determination of changes in the flux density along the three easy magnetisation axes of the iron crystal. This approach simplifies the modelling of the magnetisation process for any direction on the sheet plane because there is no need to store magnetisation loops for all possible directions in the computer memory.

To properly select the correction coefficients that allow the determination of changes in the flux density along the easy magnetisation axes for any magnetisation direction, only the hysteresis limiting loops for a few selected magnetisation directions should be measured.

Assuming that the flux density changes along the easy magnetisation axes are the basis for modelling the magnetisation processes in transformer sheets, it is easy to determine the resultant flux density vector, which cannot be measured. This vector is the sum of the flux density along the rolling direction and the flux densities along the easy magnetisation axes, which form a 45° angle with respect to the sheet plane.

Due to the Goss texture, the magnetic field strength and flux density vectors are co-linear only for magnetization along the rolling direction or transverse direction of the given transformer sheet. Then the hysteresis losses are equal to the area of the hysteresis loop for one of these directions. In other cases, hysteresis losses, especially in the corners and areas of T-joint points of the transformer cores, should be determined using the general formula on hysteresis losses for any magnetization process [8, 32]. As mentioned in the introduction, the magnetic hysteresis can be taken into account in the methods based on the integral form of Maxwell's equations. The dependences between the magnetic flux density and field strength for individual elementary segments of the division of the magnetic field area are introduced into the equations of the magnetic field distribution [29].

References

[1] Mousavi S., Shamei M., Siadatan A., Nabizadeh F., Mirimani S.H., *Calculation of Power Transformer Losses by Finite Element Method*, IEEE Electrical Power and Energy Conference, EPEC (2018), DOI: 10.1109/EPEC.2018.8598292.

[2] Sarac V., *FEM 2D and 3D design of transformer for core losses computation*, International Scientific Journal – Machines. Technologies. Materials., vol. 2, no. 3, pp. 119–122 (2017).

[3] Jain S.A., Pandya A.A., *Three Phase Power Transformer Modeling Using FEM for Accurate Prediction of Core and Winding Loss*, International Conference on Research and Innovations in Science, Engineering & Technology, Selected Papers in Engineering, vol. 1, pp. 75–80 (2017), DOI: 10.29007/z82m.

[4] Mikula L., Ramdane B., Blatter Martinho L., Kedous-Lebouc A., Meunier G., *Numerical modelling of static hysteresis phenomena using a vector extension of the Loss Surface model*, IEEE Conference on Electromagnetic Field Computation, CEFC (2022), DOI: 10.1109/CEFC55061.2022.9940905.

[5] Baron B., Kolańska-Płuska J., Łukaniszyn M., Spałek D., Kraszewski T., *Solution of nonlinear stiff differential equations for a three-phase no-load transformer using a Runge–Kutta implicit method*, Archives of Electrical Engineering, vol. 71, no. 4, pp. 1081–1106 (2022), DOI: 10.24425/aee.2022.142126.

[6] Mazgaj W., *Direct calculation of the flux density and eddy current density in the analysis of a three-dimensional electromagnetic field*, Archives of Electrical Engineering, vol. 57, no. 223, pp. 23–40 (2008).

[7] Mazgaj W., Szular Z., Szczurek P., *Calculations of magnetic field in dynamo sheets taking into account their texture*, Open Physics, vol. 15, pp. 1034–1038 (2017), DOI: 10.1515/phys-2017-0129.

[8] Pfutzner H., *Rotational Magnetization and Rotational Losses of Grain Oriented Silicon Steel Sheets – Fundamental Aspects and Theory*, IEEE Transactions on Magnetics, vol. 30, no. 5, pp. 2802–2807 (1994), DOI: 10.1109/20.312522.

[9] Pfutzner H., Mulasalihovic E., Yamaguchi H., Sabic D., Shilyashki G., Hofbauer F., *Rotational magnetization in transformer cores - a review*, IEEE Transactions on Magnetics, vol. 47, no. 11, pp. 4523–4533 (2011), DOI: 10.1109/TMAG.2011.2151201.

[10] Fiorillo L., Dupré R., Appino C., Rietto A.M., *Comprehensive model of magnetization curve, hysteresis loops, and losses in any direction in grain-oriented Fe–Si*, IEEE Transactions on Magnetics, vol. 38, no. 3, pp. 1467–1475 (2002), DOI: 10.1109/20.999119.

[11] Brailsford F., *Physicasl principles of magnetism*, D.Van Nostrand, London (1966).

[12] Bozorth R.M., *Ferromagnetism*, IEEE Press, New York (1978).

[13] Jiles D., *Introduction to magnetism and magnetic materials*, Chapman & Hall, London (1998).

[14] Soiński M., Moses A.J., *Handbook of magnetic materials*, vol. 8, Elsevier Science B.V. (1994).

[15] Shin S., Schaefer R., DeCooman B.C., *Anisotropic magnetic properties and domain structure in Fe-3%Si(110) steel sheet*, Journal of Applied Physics, vol. 109, no. 7, 07A307 (2011), DOI: 10.1063/1.3535547.

[16] Sudo M., Matsuo T., *Magnetization modeling of silicon steel using a simplified domain structure model*, Journal of Applied Physics, vol. 111, no. 7, 07D107 (2012), DOI: 10.1063/1.3672073.

[17] Furuya A., Fujisaki J., Uehara Y., Shimizu K., Oshima H., Matsuo., *Micromagnetic Hysteresis Model Dealing with Magnetization Flip Motion for Grain-Oriented Silicon Steel*, IEEE Transactions on Magnetics, vol. 50, no. 11 (2014), DOI: 10.1109/TMAG.2014.2329679.

[18] Ito S., Mifune T., Matsuo T., Kaido C., *Macroscopic magnetization modeling of silicon steel sheets using an assembly of six-domain particles*, Journal of Applied Physics, vol. 117, no. 17, 17D126 (2015), DOI: 10.1063/1.4915105.

[19] Ferreira da Luz M.V., Leite J.V., Benabou A., Sadowski N., *Three-Phase Transformer Modeling Using a Vector Hysteresis Model and Including the Eddy Current and the Anomalous Losses*, IEEE Transactions on Magnetics, vol. 46, no. 8, pp. 3201–3204 (2010), DOI: 10.1109/TMAG.2010.2049006.

[20] Sande H.V., Boonen T., Podoleanu I., Henrotte F., Hameyer K., *Simulation of a Three-Phase Transformer Using an Improved Anisotropy Model*, IEEE Transactions on Magnetics, vol. 40, no. 2, pp. 850–855 (2004), DOI: 10.1109/TMAG.2004.825004.

[21] Cardelli E., Faba A., Laudani A., Pompei M., *A challenging hysteresis operator for the simulation of Goss-textured magnetic materials*, Journal of Magnetism and Magnetic Materials, vol. 432, pp. 14–32 (2017), DOI: 10.1016/j.jmmm.2017.01.068.

[22] Demenko A., *Three Dimensional Eddy Current Calculation Using Reluctance-Conductance Network Formed by Means of FE Method*, IEEE Transactions on Magnetics, vol. 36, no. 4, pp. 741–745 (2000), DOI: 10.1109/20.877554.

[23] Theocharis A.D., Milias-Argitis J., Zacharias T., *Three-Phase Transformer Model Including Magnetic Hysteresis and Eddy Currents Effects*, IEEE Transactions on Power Delivery, vol. 24, no. 3, pp. 1284–1294 (2009), DOI: 10.1109/TPWRD.2009.2022671.

[24] Cao D., Zhao W., Liu T., Wang Y., *Magneto-Electric Coupling Network Model for Reduction of PM Eddy Current Loss in Flux-Switching Permanent Magnet Machine*, IEEE Transactions on Industrial Electronics, vol. 69, no. 2, pp. 1189–1199 (2022), DOI: 10.1109/TIE.2021.3055169.

[25] Li W., Kim I.H., Jang S.M., Koh C.S., *Hysteresis Modeling for Electrical Steel Sheets Using Improved Vector Jiles-Atherton Hysteresis Model*, IEEE Transactions on Magnetics, vol. 47, no. 10, pp. 3821–3824 (2011), DOI: 10.1109/TMAG.2011.2158296.

[26] Cardelli E., Della Torre E., Faba A., *Numerical Modeling of Hysteresis in Si-Fe Steels*, IEEE Transactions on Magnetics, vol. 50, no. 2 (2014), DOI: 10.1109/TMAG.2013.2284292.

[27] Baghel A.P.S., Kulkarni S.V., *Hysteresis modeling of the grain-oriented laminations with inclusion of crystalline and textured structure in a modified Jiles-Atherton model*, Journal of Applied Physics, vol. 113, 043908 (2013), DOI: 10.1063/1.4788806.

[28] Liorzou F., Phelps B., Atherton D., *Macroscopic Models of Magnetization*, IEEE Transactions on Magnetics, vol. 36, no. 2, pp. 418–428 (2000), DOI: 10.1109/20.825802.

[29] Mazgaj W., Sierzega M., Szular Z., *Approximation of Hysteresis Changes in Electrical Steel Sheets*, Energies, vol. 14, no. 14 (2021), DOI: 10.3390/en14144110.

[30] Mao W., Atherton D.L., *Magnetization Vector Directions in a Steel Cube*, IEEE Transactions on Magnetics, vol. 36, no. 5, pp. 3084–3086 (2000), DOI: 10.1109/20.908688.

[31] Yu Y., Atherton D.L., *Study of Magnetization Vector Rotation Process Using Tensor Magnetic Hysteresis Loops*, IEEE Transactions on Magnetics, vol. 33, no. 5, pp. 3990–3992 (1997), DOI: 10.1109/20.619639.

[32] Attalah K., Howe D., *Calculation of the rotational power loss in electrical steel laminations from measured H and B*, IEEE Transactions on Magnetics, vol. 29, no. 6, pp. 3547–3549 (1993), DOI: 10.1109/20.281225.